Electron Energy Loss Spectroscopy of the Outer Valence Shells of Acetonitrile and Methyl Isocyanide

M. Gochel-Dupuis,*,† J. Delwiche,†,‡ M.-J. Hubin-Franskin,†,‡ J. E. Collin,† F. Edard,§ and M. Tronc§

Contribution from the Laboratoire de Spectroscopie d'Electrons Diffusés, Université de Liège, Institut de Chimie B6, Sart Tilman par 4000 Liege 1, Belgique, and Laboratoire de Chimie Physique, Université P. et M. Curie, 11, Rue P. et M. Curie, 75231 Paris Cêdex 05, France.
Received October 31, 1989

Abstract: Valence-shell electronic excitation of acetonitrile and methyl isocyanide has been measured by electron energy loss spectroscopy at 20-, 25-, and 70-eV impact energies. The acetonitrile spectra are discussed in terms of valence-state excitation in the 5–9.5-eV region and of Rydberg series converging to the first and to the second ionization limits for the 9.5–12-eV energy loss range. For some of these transitions new assignments are proposed. The relative differential cross sections for the most intense Rydberg transitions have been measured as a function of the scattering angle (6–90°). They lead to a discussion of the symmetry of the excited orbitals. The spectrum of methyl isocyanide has been recorded in the 6–13-eV region at 25 eV and 2°. Only the valence region has been discussed. A previously unreported absorption band is observed at 6 eV; it is tentatively assigned to a singlet–triplet transition.

Acetonitrile and methyl isocyanide, like hydrogen cyanide, have been identified via radio techniques in comets[1] and interstellar medium,[2] as well as in the high atmosphere.[3] These molecules can be regarded as important starting compounds in chemical reactions leading to the formation of the complex species observed in the interstellar medium. Electronic spectroscopy of the CN-containing molecules has been the object of only a few studies by photon absorption, as well as by electron impact.

Concerning the acetonitrile spectroscopy, the photoabsorption spectrum is composed of two regions, one of very low intensity between 5 and 9.5 eV and the other one above 9.5 eV consisting of many fine features superimposed to an absorption continuum. A broad, low-intensity band centered at 60 000 cm^{-1} (7.43 eV) was identified by Herzberg and Scheibe.[4] Later work by Cutler[5] uncovered several bands with origins at 77 374, 86 953, and 90 853 cm^{-1}, which were thought to be the members of a Rydberg series converging to the first ionization limit.[6,7] More recently, Nuth and Glicker[8] reported quite numerous bands between 8.85 and 13.0 eV, which were interpreted as terms of four Rydberg series ($p\sigma$, $p\pi$, $d\sigma$, $s\sigma$) converging to the first ionization limit (12.21 eV) and three series ($p\sigma$, $p\pi$, $p\sigma$) converging to the second ionization limit (13.14 eV). The photoionization efficiency curve[9] reveals the presence of an $ns\sigma$ ($n \geq 5$) and an $nd\sigma$ ($n \geq 4$) Rydberg series converging to the first excited state of the ion and of an ns series ($\delta = 1.06$) converging to the third ionization limit. As the photoabsorption and photodissociation cross sections have quite similar shapes, all the discrete states lying between 8.3 and 11.4 eV are predissociated through dissociation continua, which are also responsible for the absorption continuum observed in the spectrum.[10]

By electron impact, the 5–14-eV electron energy loss spectrum of CH_3CN has been reported first by Stradling and Loudon[11] at 70-eV impact energy and zero scattering angle, with a resolution of 100 meV. Due to the limited resolution, only the first members of the three Rydberg series converging to 12.21 eV were resolved. The n_N–π^* 7.4-eV transition was observed as well as two valence states at 6.1 and 8.2 eV, which were assigned as triplets. In 1978, with a higher resolution (45–55 meV) and under nearly optical excitation conditions, Fridh[12] resolved numerous fine peaks in the 9.5–13-eV region. Most of these features have been attributed to excitation of the first members of $np\sigma$, $np\pi$, $nd\sigma$, and $ns\sigma$ Rydberg series converging toward 12.21 eV; the other ones have been assigned to members of $np\sigma$, $np\pi$, and $nd\sigma$ series converging to the second ionization limit at 13.14 eV.[7] More recently, Rianda and al.[13] studied the 4.6–11.6-eV spectrum at medium- and low-impact energies and various scattering angles (10–80°) with 60–90-meV resolution. Below 9.3 eV, they reported π–π^* and n–π^* singlet valence transitions and their triplet components. They have assigned all the peaks in the 9.3–13-eV region to $np\sigma$, $np\pi$, $nd\sigma$, and $nd\pi$ Rydberg orbitals excitation in agreement with the previous observations of Fridh.[12] In addition, on the basis of the shape of the angular differential cross sections, they discussed the singlet–triplet character of four transitions located at 5.2–7.5, 8.1, 8.96, and 10.75 eV, respectively.

Methyl isocyanide spectroscopy is known even less. Study of the electron energy loss spectrum under nearly optical excitation conditions[12] showed no absorption band below 7 eV and showed numerous fine features between 7 and 12 eV assigned to transitions to Rydberg states and members of series converging to the first and second ionization limits. Assignments in the valence region were helped with the use of HAM/3 calculations.[12]

As only medium- and low-resolution studies have been made by electron impact spectroscopy, the excitation spectrum of CH_3CN has been revisited in the energy loss range of 5–12 eV with a higher resolution. Measurements have been made at 70-, 25-, and 20-eV impact energies. In addition, the differential cross sections of the most intense Rydberg transitions are reported at various angles. Their shapes lead us to discuss the spectroscopic term of the involved states. Thanks to higher resolution, additional

* To whom correspondence should be addressed.
† Université de Liège.
‡ Maitre de Recherches, FNRS, Belgium.
§ Université P. et M. Curie.

(1) (a) Snyder, L. E.; Buhl, D. *Astrophys. J.* **1971**, *L47*, 163. (b) Huebner, W. F.; Snyder, L. E.; Buhl, D. *Icarus* **1974**, *23*, 580.
(2) (a) Solomon, P. M.; Jefferts, K. B.; Penzias, A. A.; Wilson, R. W. *Astrophys. J.* **1971**, *L107*, 168. (b) Ulich, B. L.; Conkling, E. K. *Nature* **1974**, *121*, 248.
(3) (a) Arys, E.; Nevejans, D.; Frederick, P.; Ingels, J. *Ann. Geophys.* **1983**, *1*, 163–168. (b) Arys, E.; Nevejans, D.; Ingels, J. *Nature* **1983**, *383*, 314–316.
(4) Herzberg, G.; Scheibe, G. *Z. Phys. Chem.* **1930**, *B7*, 390–406.
(5) Cutler, J. A. *J. Chem. Phys.* **1948**, *16*, 136–140.
(6) Lake, R. F.; Thompson, H. *Proc. R. Soc. London* **1970**, *A317*, 187–191.
(7) Turner, D. W.; Baker, C.; Baker, A. D.; Brundle, C. R. *Molecular Photoelectron Spectroscopy*; Wiley: New York, 1970.
(8) Nuth, J. A.; Glicker, S. *J. Quantum Spectrosc. Radiat. Transfer* **1982**, *28*, 223–231.
(9) Rider, D. M.; Ray, G. W.; Darland, E. J.; Leroi, J. *J. Chem. Phys.* **1981**, *74*, 1652–1660.
(10) Suto, M.; Lee, L. C. *J. Geophys. Res., D: Atmos.* **1985**, *90*, 13037–13040.
(11) Stradling, R. S.; Loudon, A. G. *J. Chem. Soc., Faraday Trans. 2* **1977**, *73*, 623–629.
(12) Fridh, C. *J. Chem. Soc., Faraday Trans. 2* **1978**, *74*, 2193–2203.
(13) Rianda, R.; Frueholz, R. P.; Kuppermann, A. *J. Chem. Phys.* **1984**, *80*, 4035–4043.

0002-7863/90/1512-5425$02.50/0

members of Rydberg series are resolved, leading to new insight on previous assignments.

The electron energy loss spectrum of CH_3NC has been measured in the 6–13-eV region at 25 eV and 2°. The discussion has been limited to the valence region as the resolution of the spectrum is quite similar to that in Fridh's study.[12]

Finally, the $\pi-\pi^*$ triplet excitation energies and the singlet–triplet splitting for $\pi-\pi^*$ transitions are compared within a series of triple-bond molecules such as C_2H_2, CH_3CCH, HCN, CH_3CN, and CH_3NC.

Experimental Section

The acetonitrile measurements in the Rydberg region have been performed at Université of Liège with a commercial electron spectrometer, VG LEELS 400, adapted for the analysis of gaseous targets and described in detail in a previous paper.[14] The spectrometer consists of an electron gun, an electrostatic monochromator, a collision region, and an analyzer of the same type as the monochromator. Both electron analyzers have been operated in the constant-resolution mode. The signal is detected by an electron multiplier of the channeltron type. The analyzer is rotatable from −15° to +120° around the incident direction in a plane perpendicular to the gas beam. The gaseous sample is introduced through an hypodermic needle and intersects the electron beam at 90°.

The pressure is maintained below 2×10^{-8} Torr by means of a 3000 L s^{-1} cryogenic pump. It rises to 10^{-5} Torr when the gas is admitted into the vacuum vessel.

The spectra have been recorded in the energy loss mode. They have been calibrated with the elastically scattered electrons peak as the reference. The energy resolution has been set at 22 meV for the low-angle spectra and at about 40 meV for the high-angle ones.

The acetonitrile measurements in the valence region and the methyl isocyanide spectrum have been obtained at the Université P. et M. Curie of Paris with an electron spectrometer quite similar to the one at Université of Liege and described in detail previously;[15] the overall resolution was 30 meV.

The CH_3CN samples were obtained commercially (Aldrich Chemical Co., spectrophotometric grade, purity better than 99.0%; Prolabo, 99.7% stated purity) and used without further purification other than repeated freeze–pump–thaw cycles to remove dissolved gases. The CH_3NC sample was synthesized according to standard procedure and purified prior to spectral acquisition.[16]

Electronic Configuration

Acetonitrile and methyl isocyanide are 22-electron molecules for which the ground electronic state belongs to the C_{3v} symmetry group. The electronic configuration for $\tilde{X}\ ^1A_1$ of acetonitrile is the follwowing:[17-19] $(1a_1)^2(2a_1)^2(3a_1)^2(4a_1)^2(5a_1)^2(6a_1)^2(1e)^4(7a_1)^2(2e)^4$. For methyl isocyanide, the energetic order of the $7a_1$ and 2e orbitals has been shown to be reversed.[20] The lowest energy unoccupied molecular orbitals are predicted[17,21] to be the 3e antibonding π^*_{CN} and the $8a_1$ antibonding σ^*_{CC} and/or σ^*_{CH} valence[21] orbitals for both molecules. Excitation of an electron from an e to an e or a_1 orbital leads to A_1, A_2, E, or E states, while transition from an a_1 to an e or a_1 orbital leads to E or A_1 states.

The Rydberg series will be $ns a_1$, $np a_1$, npe, $nd a_1$, and nde corresponding to $ns\sigma$, $np\sigma$, $np\pi$, $nd\sigma$, and $nd\pi$ and $nd\delta$ series, respectively, in the pseudodiatomic model with the z axis on the CN internuclear axis.[22]

Transitions from $\tilde{X}\ ^1A_1$ to $^1A_2$ states are optically forbidden but allowed by magnetic dipole selection rules;[23] they correspond to $\Sigma^- - \Sigma^+$ in the $C_{\infty v}$ symmetry point group. Excitation of $^1A_1$ and ^1E states is optically allowed in the same manner as the $^1\Sigma^+ - ^1\Sigma^+$ and $^1\Pi - ^1\Sigma^+$ transitions in the $C_{\infty v}$ symmetry point group, respectively.

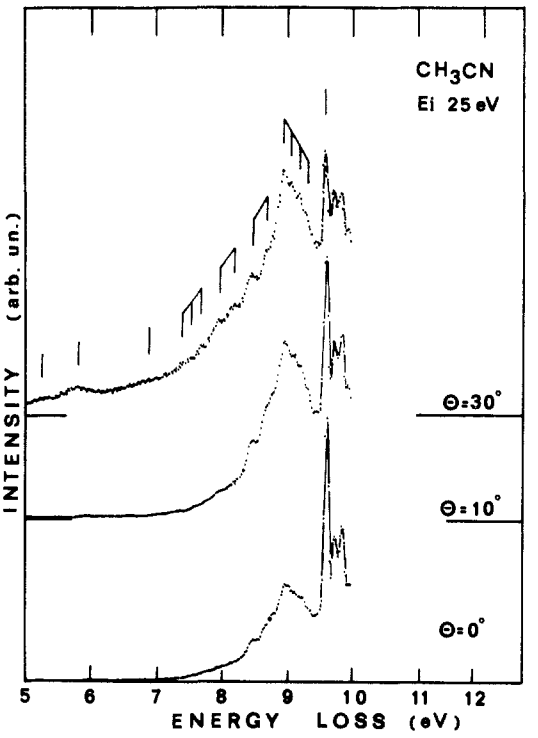

Figure 1. Electron energy loss spectra of acetonitrile in the valence region. The impact energy is 25 eV, and the scattering angles are 0°, 10°, and 30°.

Table I. Valence-Shell Excited States of CH_3CN Below the 9.589-eV 3pλ Rydberg State

transition	state sym. $C_{\infty v}$	state sym. C_{3v}	HAM/3 calcd[a]	previous exptl results b	previous exptl results a	previous exptl results c	this work
2e → 3e ($\pi \rightarrow \pi^*$)	$^3\Sigma^+$	$^3A_1$	7.2	6.1		5.2	5.8
	$^3\Delta$	^3E	7.8				6.8
	$^{1,3}\Sigma^-$	$^{1,3}A_2$	8.3	8.2		8.1	8.20
	$^1\Delta$	^1E	8.8		8.45	8.45	8.44
						8.64	8.66
						8.72	
	$^1\Sigma^+$	$^1A_1$	11.9		11.26		9.8
$7a_1 \rightarrow 3e$ ($n_N \rightarrow \pi^*$)	$^3\Pi$	^3E				7.7	7.4
							7.55
							7.68
	$^1\Pi$	^1E	10.1	9.04	9.2	8.96	8.96
						9.11	9.10
						9.21	9.20
							9.30

[a] Reference 12. [b] Reference 11. [c] Reference 13.

Results and Discussion

A. Acetonitrile. A.1. Valence Region. The electron energy loss spectrum of CH_3CN in the valence region is shown in Figure 1. Incident electron energy was fixed at 25 eV and the scattering angle at 0°, 10°, and 30°, to allow the momentum transfer K to be small and to vary from 0.13 to 0.27 au in the forward scattering spectrum, up to 0.7 au in the 30° one. Such experimental conditions favor symmetry-allowed transitions, together with spin-forbidden transitions (singlet–triplet) at the higher angle.

All spectra are intensity-normalized on that of the Rydberg transition at 9.589 eV, first term of an $np\lambda$ series; they are in general agreement with previous results.[12,13]

The excitation energies are reported in Table I together with previous experimental results and HAM/3 theoretical calculations. Assignment is difficult because of overlapping broad bands and limited energy resolution making vibrational structures poorly

(14) Furlan, M.; Hubin-Franskin, M. J.; Delwiche, J.; Roy, D.; Collin, J. E. *J. Chem. Phys.* **1985**, *82*, 1797–1803.
(15) Ben Arfa, M.; Tronc, M. *J. Chim. Phys.* **1988**, *85*, 879–897.
(16) Corey, E. J. *Organic Syntheses* **1966**, *46*, 75.
(17) Snyder, L. C.; Bosch, A. *Molecular wave functions and properties*; Wiley: New York, 1972; pp T162–T168.
(18) Cambi, R.; Von Niessen, W. *J. Electron Spectrosc. Relat. Phenom.* **1987**, *42*, 245–253.
(19) Asbrink, L.; Von Niessen, W.; Bieri, G. *J. Electron Spectrosc. Relat. Phenom.* **1980**, *21*, 93–101.
(20) Tae-Kyu, H. *J. Mol. Struct.* **1972**, *11*, 185–189.
(21) Edard, F.; Hitchcock, A.; Tronc, M. *J. Phys. Chem.* **1990**, *94*, 2768–2774.
(22) Lindholm, E. *Ark. Phys.* **1969**, *40*, 125.
(23) Herzberg, G. *Molecular spectra and molecular structure III. Electronic Spectra and Electronic Structure of Polyatomic Molecules*; Van Nostrand: New York, 1966; p 134.

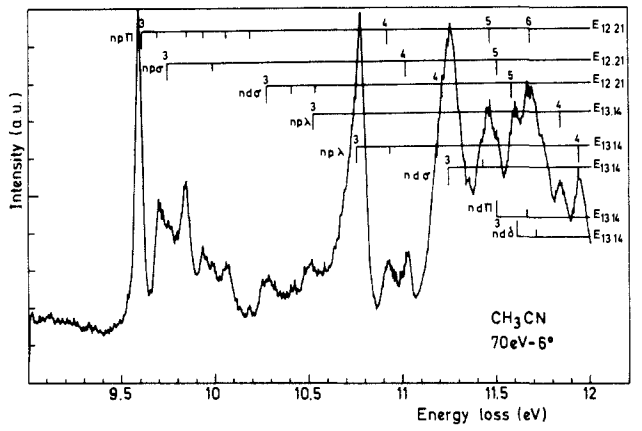

Figure 2. Electron energy loss spectrum of acetonitrile in the 9–12-eV region at 70 eV and 6°. The Rydberg series converging to the 12.21- and 13.14-eV ionization limits are reported on the spectrum.

resolved. Moreover, the spectroscopic terms corresponding to 2e–3e (π–π^*) and $7a_1$–3e (n_N–π^*) transitions overlap. The intense feature at 8.96 eV displays 3 quanta of vibration with a 0.110-eV mean spacing attributed to excitation of the ν_7 mode (CH_3 rocking). It is assigned to the nitrogen lone pair $n_N(7a_1)$ orbital excitation into the π^*(3e) orbital, in agreement with previous results[12,13] and the UV absorption spectrum.[5] The term value (4.18 eV) of this $^1\Pi$ state is smaller than the corresponding one for the excitation of $1s_c$ and $1s_N$ electrons to empty π^* (5.5–5.7 eV) as recently observed in inner-shell electron energy loss spectroscopy,[24] as expected because of the greater localization of the core hole orbitals.[25] The 7.95- and 8.44-eV structures with their associated ν_2 vibrational modes at, respectively, 0.22 and 0.25 eV (CN stretching) are understood as symmetry-allowed components of the π–π^* transition (2e–3e). The corresponding term values of 3.6 and 4.3 eV are again smaller than for the inner-shell $(1s_C)^{-1}\pi^*$ and $(1s_N)^{-1}\pi^*$ states.

All small-intensity extra structures that appear clearly on the 30° spectrum at 5.3–5.5, 6.8, and 7.4 eV are attributed to triplet states. The intensity of the 5.8-eV band is nearly constant in the 30–120° scattering angle range in agreement with results of Rianda et al.,[13] confirming the spin-forbidden nature of the involved transition. The other triplet states are difficult to analyze because they strongly overlap with singlet states. The term values of these triplet states (5.4–5.7 eV) are very similar to those of the singlet inner-shell excited states to the same final π^* orbital (5.5–5.7 eV), as first suggested by Friedrich and al.,[25] mainly because the exchange integral is absent for singlet–triplet transitions and is very small for an initial core hole.

According to Fridh,[12] excitation of the (2e–3e) $^1\Sigma^+$ valence state would be responsible for some features observed between 11.26 and 11.8 eV. However, the relative intensity of these peaks does not vary in the same manner when the impact energy is varied or the scattering angle increased. The HAM/3 calculations have been shown in many cases to overestimate the Σ^+ singlet–triplet splitting; in CO_2, another 22-electron molecule, the discrepancy is about 1.5 eV.[27-29] Thus, we suggest that, in CH_3CN, the Σ^+ manifests itselfs as a broad band underlying the 3pλ Rydberg feature at 9.589 eV and centered at 9.8 eV. Then the singlet–triplet splitting would be about 3.6 eV. This suggestion is confirmed by comparison with S–T splitting for Σ^+ states in triple-bonded molecules as discussed further in this paper.

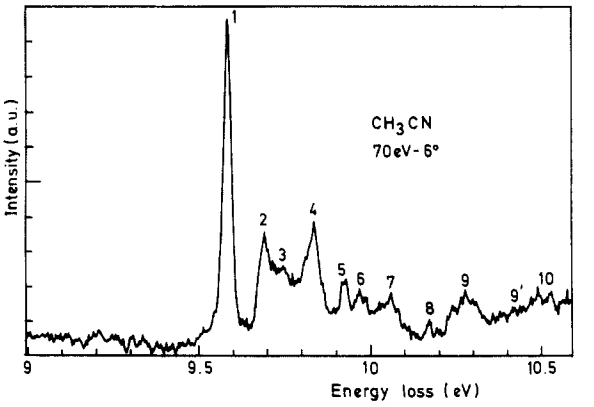

Figure 3. Deconvoluted 70 eV and 6° electron energy loss spectrum of acetonitrile in the 9–10.6-eV region. The numbers 1–10 are used as labels for the various features.

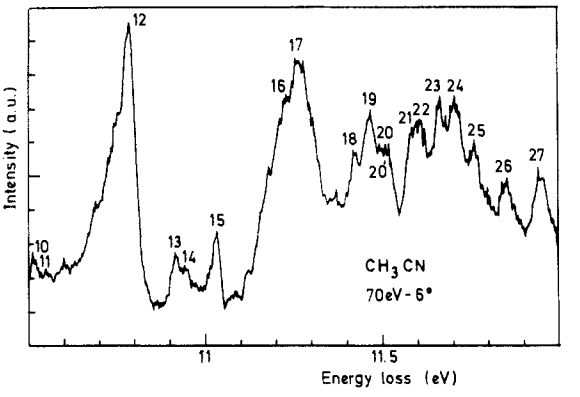

Figure 4. Deconvoluted 70 eV and 6° electron energy loss spectrum of acetonitrile in the 10.5–12-eV region. The numbers 10–27 are used as labels for the various features.

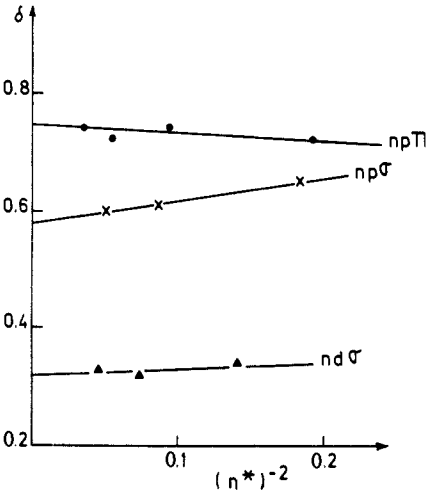

Figure 5. Edlen's diagrams giving the variation of the quantum defect (δ_Λ) with the reduced term energies n^{*2} for the first terms of the Rydberg series converging to the first ionization limit (12.21 eV). It has been plotted on the basis of our interpretation.

A.2. Rydberg Series and the 9–12-eV Region. The 9–12-eV energy loss spectrum recorded at 70 eV and 6° is shown in Figure 2. It is largely dominated by numerous isolated features superimposed to a continuum especially between 11 and 12 eV.

As shown in Figures 3 and 4 deconvolution[30] of the spectrum helped to determine more precisely the energy values of poorly resolved features, particularly in the 11–12-eV region. The energy values of all the peaks are listed in Table II where they are

(24) Hitchcock, A. P.; Tronc, M.; Modelli, A. *J. Phys. Chem.* **1989**, *93*, 3069–3077.
(25) Friedrich, H.; Sonntag, B.; Rabe, P.; Butscher, N.; Schwartz, W. H. E. *Chem. Phys. Lett.* **1979**, *64*, 360–366.
(26) Åsbrink, L.; Fridh, C.; Lindholm, E. *Chem. Phys.* **1978**, *27*, 159–168.
(27) Hubin-Franskin, M. J.; Delwiche, J.; Leclerc, B.; Roy, D. *J. Phys. B: At. Mol. Opt. Phys.* **1988**, *21*, 3211–3229.
(28) Cossart-Magos, C.; Jungen, M.; Launay, F. *Mol. Phys.* **1987**, *61*, 1077–1117.
(29) Winter, N. W.; Bender, C. F.; Goddard, W. A. *Chem. Phys. Lett.* **1973**, *20*, 489–492.

(30) Allen, J. D.; Grimm, F. A. *Chem. Phys. Lett.* **1979**, *66*, 72–78.

Table II. Energy Values (eV) of the Transitions Observed in the 9–12-eV Region

optical spectra		electron energy loss spectroscopy						
					this work			
Nuth et al.[8]	Cutler[5]	Stradling et al.[11]	Fridh[12]	Rianda et al.[13]	70 eV, 6°[a]	20 eV, 6°	20 eV, 10°	20 eV, 15°
9.595	9.59		9.594	9.58	9.589[1]	9.592	9.595	9.596
9.678		9.63						
9.695	9.69		9.704		9.694[2]	9.700	9.699	9.700
9.716	9.71			9.71				
	9.74				9.745[3]			
	9.78							
	9.83	9.82						
9.842	9.84		9.842	9.80	9.838[4]		9.839	9.836
9.935	9.93		9.940	9.95	9.929[5]	9.928	9.931	9.928
9.983			9.991		9.973[6]			
10.056	10.07	10.04	10.064	10.03	10.060[7]	10.057	10.055	10.054
10.181			10.181		10.182[8]			
10.292			10.292	10.29	10.286[9]	10.280	10.283	10.280
					10.415[9]			
10.501		10.52	10.496	10.541	10.520[10]		10.516	10.512
10.744		10.744	10.73	10.75	10.531[11]			
10.774								
10.778	10.78		10.775		10.780[12]	10.776	10.781	10.776
10.918			10.917		10.916[13]			
10.941		10.95		10.94	10.937[14]	10.936	10.941	10.940
11.007								
11.027			11.025		11.029[15]	11.028		
11.177								
11.220			11.215		11.220[16]			
11.266	11.26			11.25	11.268[17]	11.260	11.260	11.260
11.307								
11.345		11.34						
11.374								
11.416					11.422[18]			
11.465				11.46	11.467[19]	11.464	11.463	11.464
11.491					11.503[20]			
11.512					11.516[20]			
11.578					11.587[21]			
11.590			11.594		11.602[22]			
11.607		11.60						
11.666		11.67		11.68	11.662[23]			
11.701					11.704[24]			
11.717								
11.745			11.758		11.759[25]			
11.808		11.81						
11.849					11.85[26]			
11.926								
11.940			11.946	11.94	11.947[27]			

[a] The superscript numbers are used as labels for the features appearing in Figures 3 and 4.

compared with those of the literature. Our data are in quite good agreement with previous electron impact studies[11-13] and with optical spectroscopy data.[8]

The spectrum is dominated by excitation of Rydberg series converging to the first and to the second ionization limits.[7] In order to help interpretation and classification of the Rydberg series, Edlen's diagrams have been established as shown in Figures 5 and 6. We have plotted the variation of the quantum defect ($\delta_{l\lambda}$) with the reduced term energies $(n^*)^{-2} = (n-\delta)^{-2}$. According to the commonly accepted Rydberg–Ritz formula[31] $\delta_{l\lambda} = \alpha_{l\lambda} + \beta_{l\lambda}(n^*)^{-2}$, diagrams of $\delta_{l\lambda}$ as a function of $(n^*)^{-2}$ should give straight lines analogous to atomic Edlen's plots.[32]

A.2.1. Series Converging to the First Ionization Limit (12.21 eV). The lowest energy peak at 9.589 eV (peak 1, Figure 3) is to be attributed to the excitation of the $n = 3$ term of the 2e–3pλ series with a quantum defect $\delta = 0.73$ in agreement with Nuth and Glicker[8] (Table III). This electronic transition is accompanied by excitation of the ν_4 and ν_2 vibrational modes. The frequencies are quite similar to those of the ion in its ground state ($\nu_4 = 0.11$ eV, $\nu_2 = 0.249$ eV[7]). In addition, the relative intensities of the vibrational components are the same as in the photoelectron spectrum.[7] These observations confirm the Rydberg character of the transition. The second term of the series is located at 10.916 eV (peak 13) with a quantum defect $\delta = 0.74$. The third and fourth terms are very likely observed as features 19 and 24 at 11.467 and 11.704 eV superimposed on the broad continuum lying between 11 and 12 eV.

Table III. Rydberg Series Converging to the First Ionization Limit (12.21 eV; $\nu_2 = 0.249$ eV; $\nu_4 = 0.11$ eV)[7]

n	E (eV)	δ	n	E (eV)	δ
3	9.589	0.72	3	9.745	0.65
$3 + \nu_4$	9.694	0.72	$3 + \nu_2$	9.973	
$3 + \nu_2$	9.838	0.72	4	11.029	0.61
$3 + \nu_2 + \nu_4$	9.929	0.72	5	11.516	0.62
$3 + 2\nu_2$	10.060	0.72	3	10.286	0.34
$3 + 2\nu_2 + \nu_4$	10.182	0.72	$3 + \nu_4$	10.415	0.34
4	10.916	0.74	$3 + \nu_2$	10.531	0.34
5	11.467	0.72	4	11.220	0.32
6	11.704	0.74	5	11.587	0.33

The poorly resolved 9.745-eV peak (peak 3) is due to the excitation of the first member of a npλ Rydberg series with $\delta = 0.65$ (Table III). Weak excitation of 1 quantum of the ν_2 mode manifests itself at 9.973 eV (peak 6) with a value of 0.228 eV, quite compatible with that reported for the ion in its $\tilde{X}$ state. Nuth and Glicker[8] suggested the first member of this series to be located at 9.678 eV, leading to a value of the ν_2 mode that is too high

(31) Born, M. *Vorlesungen über Atommechanik*; Springer-Verlag: Berlin, 1925.

(32) Edlen, B. *Encyclopedia of Physics, XXVII, Spectroscopy I*, Flügge, S., Ed.; Springer: Berlin, 1964; pp 123–130.

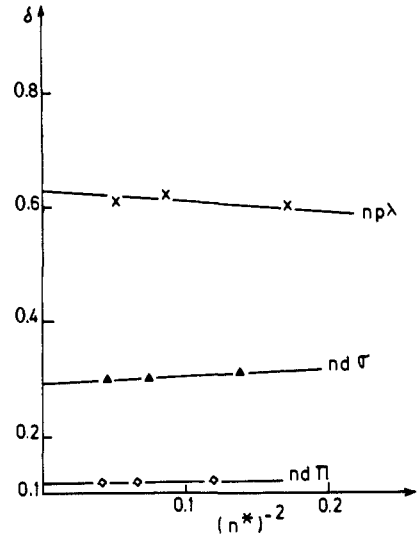

Figure 6. Edlen's diagrams giving the variation of the quantum defect ($\delta_{l\lambda}$) with the reduced term energies n^{*2} for the first members of the Rydberg series converging to the second ionization limit (13.14 eV). It has been plotted on the basis of our interpretation.

Table IV. Rydberg Series Converging to the Second Ionization Limit (13.14 eV; ν_3 = 0.16 eV)[7]

n	*E* (eV)	δ	*n*	*E* (eV)	δ
3	10.520	0.72	3	11.503	0.12
4	11.85	0.73	3 + ν_3	11.662	
3	10.780	0.60	4	12.24[a]	0.12
3 + ν_3	10.937	0.60	5	12.57[a]	0.11
4	11.947	0.62	3	11.602	0.03
5	12.44[b]	0.61	3 + ν_3	11.759	0.03
3	11.268	0.31			
3 + ν_3	11.422	0.31			
4	12.14[a]	0.30			
5	12.53[b]	0.30			

[a] Values from Rianda and al.[13] [b] Values from Fridh.[12]

(0.305 eV). The second and the third terms are observed at 11.029 eV (peak 15) and 11.516 eV (peak 20), respectively, as seen in the spectra (Figures 2 and 4; Table III).

The weak feature of peak 9 at 10.286 eV is to be assigned to the n = 3 term of an $nd\sigma(a_1)$ Rydberg series with a quantum defect δ = 0.34. It is accompanied by the excitation of 1 quantum of the ν_4 mode, leading to the 10.415-eV position, and very likely also of the ν_2 mode, the corresponding feature expected at 10.531 eV being a component of the broad 10.520-eV peak. These results are different from those of Nuth and Glicker[8] who located the $1\nu_2$ level at 10.501 eV, leading to too low a value for the vibrational energy (0.209 eV). The n = 4 and n = 5 terms are hidden by more intense transitions in the 11.22- and 11.587-eV regions, respectively.

As shown in Figure 5, the experimental Edlen's diagrams for the $nd\lambda$ and $np\lambda$ series converging to the $\tilde{X}\ ^2E$ ionic state have been plotted for members with principal quantum numbers n = 3–5 and, when resolved, 6. For each Rydberg series the variation of $\delta_{l\lambda}$ with $(n^*)^{-2}$ is quite smooth and linear, confirming the classification.

It is to worth noting that previously[8,12] the second term of an ns series starting at 8.93 eV, i.e., in the valence region, was reported at 10.744 eV. However, despite our high resolution, no feature is observed at this energy in our spectra.

A.2.2. Series Converging to the Second Ionization Limit (13.14 eV). The Rydberg series converging to the second ionization limit are located above 10.5 eV (Table IV).

In agreement with previous assignments, the broad intense peak 12 centered at 10.780 eV (Figures 2 and 4) is due to excitation of the n = 3 term of the $np\lambda$ series; the transition is accompanied by vibrational excitation of 1 quantum of the ν_3 mode, with a frequency of 0.157 eV, very close to that observed in the second band of the photoelectron spectrum (0.16 eV).[7] The second term of this series is situated at 11.947 eV (peak 27, Figures 2 and 4). The quantum defect for these two Rydberg orbitals is calculated to be 0.60.

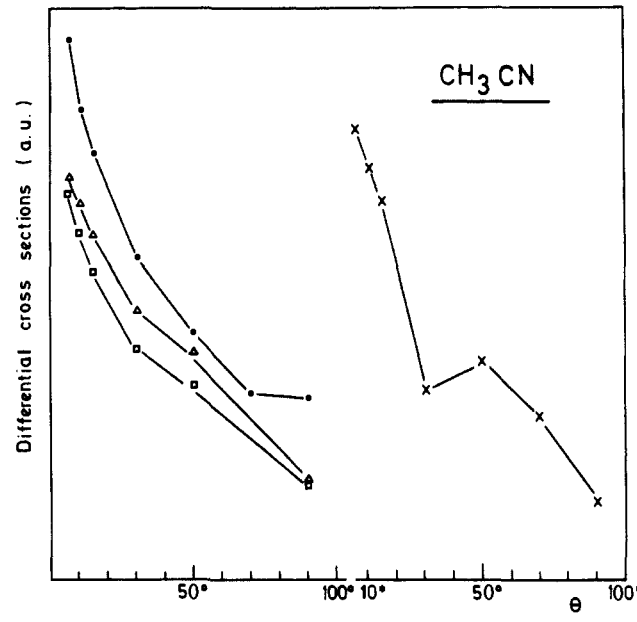

Figure 7. Relative differential cross sections at 20 eV for the elastic scattering (●) and for the 9.589-eV (×), 10.780-eV (△) and 11.268-eV (□) electronic transitions in acetonitrile.

The second intense peak (peak 17) in this region is located at 11.268 eV. It is to be assigned to the first term (n = 3) of an $nd\sigma(a_1)$ transition with a quantum defect δ = 0.31, while peak 18 at 11.422 eV corresponds to the $3d\sigma + 1\nu_3$ excitation. The n = 4 term of this series has been observed previously at 12.141 eV.[12,13] It is noted that Nuth and Glicker[8] reported the first term at 11.361 eV, in disagreement with this work and previous ones.

The low-intensity feature (peak 10) at 10.520 eV is attributed to excitation of the first member of an $np\sigma(a_1)$ series. The second term should be at 11.85 eV. This interpretation confirms the observations of Rianda and al.[13] who located the second term at 11.94 eV. However, it disagrees with that of Nuth and Glicker[8] and that of Fridh[12] (Table IV). The former authors suggest the first term should be located at 9.716 eV, leading to a quantum defect of 1.0, well too high for a "p" series. Both authors did not report the 10.520- and 11.85-eV bands. In our hypothesis, the features classified by Nuth and Glicker[8] and Fridh[12] as $4p\sigma(a_1)$ might be the first term and its $1\nu_3$ transition of a $nd\delta(e)$ series with a quantum defect δ = 0.03. It is remarkable that HAM/3 calculations predicted a valence state (2e–3e) $^1\Sigma^+$ at 11.9 eV, which Fridh claimed to be responsible of the broad peaks around 11.5 eV.

The first term of the $nd\pi(e)$ series is observed at 11.503 eV (peak 20, Figure 4) with a deduced quantum defect δ = 0.12 (Table IV). This transition is accompanied by excitation of the ν_3 mode, which is observable at 11.662 eV (peak 23). The following member is located outside the energy loss range studied in this work.

With use of this hereabove discussed classification of four series, the quantum defect $\delta_{l\lambda}$ of three series has been plotted as a function of $(n-\delta)^{-2}$. The diagrams displayed in Figure 6 exhibit quite smooth variations.

A.2.3. Angular Differential Cross Sections. The relative differential cross sections have been measured as a function of scattering angle (6–90°) at 20 eV for the elastic scattering process, as well as for the three most intense transitions observed at 9.589 eV (peak 1), 10.780 eV (peak 12), and 11.268 eV (peak 17) in the low-angle spectrum (Figure 2). They are displayed in Figure 7. Their shape is consistent with those of spin-allowed transitions.

The behavior of the elastic differential cross section and that of the 10.780-eV transition (Figure 7) are in good agreement with

Table V. Valence-Shell Excited States of CH_3NC

transition	state sym ($C_{\infty v}$)	HAM/3 calcd[a]	previous exptl results[a]	this work
$2e \rightarrow 3e$ ($\pi \rightarrow \pi^*$)	$^3\Sigma^+$	7.2		6.0[b]
				6.28
				6.50
	$^3\Delta$	7.6		
	$^{1,3}\Sigma^-$	8.1		
	$^1\Delta$	8.6		
	$^1\Sigma^+$	11.3	9	9.02
$7a_1 \rightarrow 3e$ ($n_c \rightarrow \pi^*$)	$^1\Pi$	8.9	7.8	7.82

[a] Reference 12. [b] See text section B.

those published by Rianda and al.[13]

The differential cross section of the 3pλ(a_1 or e) state located at 9.589 eV offers a peculiar shape with a minimum around 30°, which is observed at both 20 and 70 eV. It looks very similar to that for the optically symmetry-forbidden $a'^1\Sigma^+_g$–$X^1\Sigma^+_g$ transition in the nitrogen molecule.[33] As Σ^+_g species of linear molecules ($D_{\infty h}$, $C_{\infty v}$) correspond to A_1 species in C_{3v} symmetry point group to which CH_3CN belongs, the angular behavior suggests that the 9.589-eV state is of A_1 symmetry and is excited through a 2e–3pe(π^*) transition. This interpretation is in contradiction with previous assignments that, on the basis of Lindholm's considerations,[22] located $npa_1(\sigma)$ Rydberg series at lower energy than the npe(π) one, the quantum defect being assumed to be the largest one for $pa_1(\sigma)$ series.

On the basis of our interpretation for the 9.589-eV (3pe) state, the 9.745-eV transition should then correspond to excitation of a 2e electron into the $3pa_1(\sigma)$ orbital, leading to an E symmetry state.

The relative $d\sigma/d\theta$ curves for the 10.780-eV ($7a_1 \rightarrow 3pa_1$ or e) and 11.268-eV ($7a_1 \rightarrow 3da_1$) transitions (Figure 7) have quite smooth behavior as expected for symmetry-allowed transitions. According to earlier assignments,[12,13] the 10.780-eV transition has been suggested to be $7a_1 \rightarrow 3pe(\pi)$, relying on the value of the quantum defect generally expected to be lower for $p\pi$ series than for $p\sigma$ ones; in that case the state is of E symmetry. However, on the basis of the angular differential cross section, the alternative interpretation of a $3pa_1$ excited orbital might also be considered; in that case, the state should be of A_1 symmetry corresponding to Σ^+_u in $D_{\infty h}$ symmetry point group. Both interpretations are compatible with the angular behavior of the cross section. The choice of 10.780 eV involving the 3pe or $3pa_1$ orbital influences the assignment of the 10.520-eV transition, which involves then the $3pa_1$ or 3pe orbital.

The 11.268-eV state is excited through a $7a_1 \rightarrow 3da_1(\sigma)$ transition corresponding to $\Sigma^+_u \rightarrow \Sigma^+_g$ in $D_{\infty h}$ molecules; its symmetry is then A_1. This assignment relies on the angular differential cross section reported in this study and on the value of the quantum defect deduced from the energy of this Rydberg term; it confirms a previous interpretation that was based on quantum defect consideration.

A.3. Valence Predissociative States. Most of the bands in the Rydberg region, especially between 10.6 and 11.8 eV, are obviously in interaction with valence dissociative states leading to band diffuseness. Indeed, previous work by Suto and Lee[10] showed that for an absorption continuum the excited molecule will mainly decay through dissociation. The CN neutral fragment fluorescence quantum yield is the same in the region of the discrete states in the absorption continua, indicating that the discrete states are strongly predissociated through dissociation continua. This case is similar to those observed in CO_2[27,28] and could explain the broad features and the important underlying continuum we observe between 11 and 12 eV (Figure 2).

B. Methyl Isocyanide. Valence Region. The electron energy loss spectrum of methyl isocyanide, a stable isomer of acetonitrile, has been obtained at 25-eV incident energy for a 2° scattering

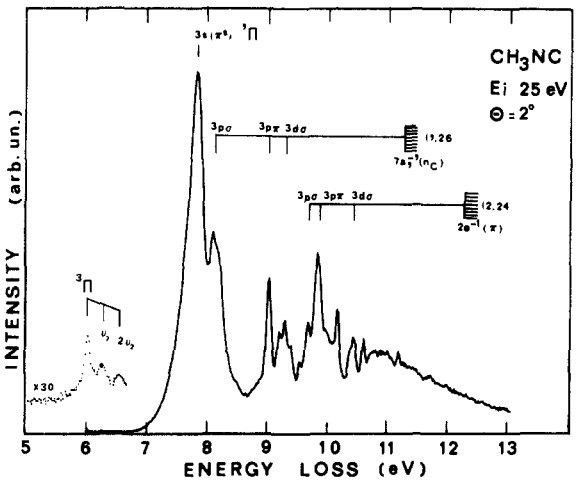

Figure 8. Electron energy loss spectrum of methyl isocyanide in the 5–13-eV region at 25 eV and 2°. The Rydberg series converging to the 11.26- and 12.24-eV ionization limits are indicated on the spectrum.

angle. As shown in Figure 8, it is in very good overall agreement with the only known electron impact spectra of Fridh[12] obtained at 45- and 500-eV energy at, respectively, 3° and 0°. But the present spectrum reveals a low-intensity structured band around 6 eV that was not observed previously. The valence excitation energies are reported in Table V and are compared to Fridh's experimental data and HAM/3 calculations.[12]

The CH_3NC energy loss spectrum appears quite different from the CH_3CN one for two reasons: First, if the binding energy of the 2e(π) is the same in the two isomers, the lone pair $n_C(7a_1)$ is less bound in CH_3NC than the lone pair n_N in CH_3CN and less bound than the 2e(π) orbital, so that valence transitions and Rydberg series converging to the $7a_1$ and 2e limits appear with a reverse order compared to CH_3CN. Second, the 3e(π^*) lowest unoccupied molecular orbital (LUMO) has a different spacial charge distribution in the two molecules, as evidenced recently in the carbon 1s and nitrogen 1s inner-shell excitation spectra, which present significant differences,[24] and also in the shape resonance decay.[21] Indeed the short-lived negative ion built on the CH_3CN or CH_3NC ground state with an extra electron in the 3e orbital leads to selective resonant vibrational excitation, which differs in the two molecules,[21] and to dissociative attachment with an intensity of C_2HN^- and $C_2H_2N^-$ ions greater by a factor of 10 in CH_3CN than in CH_3NC.[34] The delocalization of the 3e LUMO following hyperconjugation effect with the π^*-like CH_2 orbital of the methyl group appears stronger in CH_3CN than in CH_3NC.

The CH_3NC energy loss spectrum is dominated by Rydberg series converging to the first two ionization limits at 11.26 eV ($7a_1$) and 12.24 eV (2e). As the spectrum is very similar to that of Fridh,[12] we only give the first member of each series obtained with the same term values as in CH_3CN. Three series starting at 8.10 eV ($3p\sigma$), 9.02 eV ($3p\pi$), and 9.28 eV ($3d\sigma$) converge to the $7a_1$ limit, and three series starting at 9.66 eV ($3p\sigma$), 9.82 eV ($3p\pi$), and 10.40 eV ($3d\sigma$) converge to the 2e limit. The intense peak observed at 7.82 eV is attributed to the $n_C(7a_1)$–π^*(3e) transition.

Notice that its intensity is higher than the lone-pair n_N excitation in CH_3CN, in contrast to the inner-shell spectra where the $1s_C$–π^* and $1s_N$–π^* transitions have similar intensities.[24] The term value for the corresponding $^1\Pi$ state (4.45 eV) is slightly higher than in CH_3CN (4.18 eV), but smaller than the 5.7-eV term value for

(33) Cartwright, D. C.; Chutjan, A.; Trajmar, S.; Williams, W. *Phys. Rev.* **1977**, *16A*, 1013–1040.

(34) Heni, M.; Illenberger, E. *Int. J. Mass Spectrom. Ion Phen.* **1986**, *73*, 127–144.

(35) Dance, D. F.; Walker, I. C. *J. Chem. Soc., Faraday Trans. 2* **1974**, *70*, 1426–1434.

(36) Flicker, W. M.; Mosher, O. A.; Kuppermann, A. *J. Chem. Phys.* **1978**, *69*, 3311–3320.

(37) Van Veen, E. H.; Plantenga, F. L. *Chem. Phys. Lett.* **1976**, *38*, 493–497.

(38) Stradling, R. S.; Baldwin, M. A.; Loudon, A. G.; Maccoll, A. *J. Chem. Soc., Faraday Trans. 2* **1976**, *72*, 871–877.

Table VI. Triplet $\pi \rightarrow \pi^*$ Excitation Energies for Triple-Bond (C≡C, C≡N) Containing Molecules: C_2H_2, HCN, CH_3CN, CH_3NC, and CH_3CCH

	C_2H_2		CH_3CCH		HCN		CH_3CN		CH_3NC	
	HAM/3[b]	exptl[d]	HAM/3[a]	exptl[c]	HAM/3[b]	exptl[e]	HAM/3[a]	exptl[f]	HAM/3[a]	exptl[f]
$^3\Sigma^+$	5.25	5.4	6.2	5.3	6.42	5.46	7.2	5.3	7.2	
$^3\Delta$	5.82	6	6.7	5.8	7.06	5.99	7.8	6.8	7.6	6.0

[a] Reference 12. [b] Reference 26. [c] Reference 35. [d] Reference 37. [e] References 13 and references therein. [f] This work.

Table VII. Singlet-Triplet Splitting for $\pi\pi^*$ Excitations in C_2H_2, HCN, CH_3CN, CH_3NC, and CH_3CCH

	C_2H_2		CH_3CCH		HCN		CH_3CN		CH_3NC	
	HAM/3[a]	exptl[d]	HAM/3[a]	exptl[b]	HAM/3[c]	exptl[e]	HAM/3[a]	exptl[f]	HAM/3[a]	exptl[f]
$^1\Sigma^+$–$^3\Sigma^+$	4.79	3.87	4.6		4.84	3.38	4.7	3.6	4.1	3.02
$^1\Delta$–$^3\Delta$	1.14	1.3	1.	1.4	1.28		1.	1.	1.	

[a] Reference 12. [b] References 35 and 36. [c] Reference 26. [d] References 37 and 38. [e] Reference 13. [f] This work.

the inner-shell $1s^{-1}\Pi^*$ states.[24] Higher energy valence states are obscured by the Rydberg series. However, from comparison with the CH_3CN spectrum and the Π–Π^* transition energies in similar molecules, the 2e–3e transition should lie between 9 and 10 eV. The underlying continuum apparent on the low-energy side of the $3p\pi$ Rydberg state at 9.02 eV may be the optically allowed $^1\Delta$ component of this transition. The 6-eV structured band is assigned to a triplet state. The vibrational structure with a 0.250-eV mean spacing compares well with the 0.268-eV vibrational energy of the ν_2 mode (CN stretching) in the ground state. Although both the energy and singlet–triplet splitting may agree (Tables VI and VII) with a triplet component of the 2e–3e transition, the vibrational structure seems to rule out such an assignment. Thus, we prefer to attribute it as the triplet component ($^3\Pi$) of the $7a_1$–3e transition giving a $^3\Pi$–$^1\Pi$ splitting of 1.82 eV, comprised between that of the $^3\Sigma^+$–$^1\Sigma^+$ and $^3\Delta$–$^1\Delta$ splitting and quite similar to the 1.6 eV $^3\Pi$–$^1\Pi$ splitting in CH_3CN.

C. Triplet Excitation Energies and Singlet–Triplet Splitting. Triplet excitation energies for π–π^* transitions in CCH and CN triple-bond-containing molecules (acetylene, propyne, hydrogen cyanide, acetonitrile, methyl isocyanide) are reported in Table VI. All observed triplet states for the π–π^* transitions fall in the 5.3–5.5-eV region for the $^3\Sigma^+$ states and in the 5.8–6.0-eV range for the $^3\Delta$ one, roughly 1 eV lower than HAM/3 theoretical calculations.[26]

For the same series of molecules the singlet–triplet splitting with the π–π^* transition (Table VII) has a value of 3–4 eV for the Σ^+ states. The $^3\Sigma^+$–$^1\Sigma^+$ splitting of 6.0 eV in acetonitrile, obtained with an 11.26-eV energy for the singlet component[25] and a 5.2-eV value for the triplet one, looks too high. So we suggest that the singlet appears as an underlying continuum around 9.8 eV. The smaller value of 1.3–1.4 eV for the $^3\Delta$–$^1\Delta$ splitting may result from a lower localization of the Δ states.

Conclusions

The outer valence shell electron energy loss spectra of acetonitrile and methyl isocyanide have been reported at medium- and low-impact energies. They have been discussed in terms of transitions to valence states and to Rydberg ones.

In the valence region (5–9.5 eV), the assignments are in agreement with previous works. For methyl isocyanide, a new band is observed at 6 eV and tentatively assigned to a triplet state.

For both molecules the 9–12-eV excitation region is dominated by Rydberg series converging to the two lowest ionization limits. In the case of acetonitrile the Rydberg series classification has been revisited. The 11.599-eV state is suggested to be the first term of $nd\delta$ series converging to the second ionization limit, the quantum defect being 0.03. In addition, the angular behavior of the relative differential cross sections of the 9.589-, 10.780-, and 11.268-eV electronic transitions has led us to discuss the symmetry of the involved states. Indeed, the 9.589-eV transition (2e–3pλ) differential cross section exhibits a minimum at 30° and a shape quite similar to that of the symmetry-forbidden Σ^+_g–Σ^+_g transition in N_2, leading us to suggest A_1 symmetry for the excited state. Thus, the series is an $npe(\pi)$ one.

Acknowledgment. We are grateful to the Fonds National de la Recherche Scientifique of Belgium for research positions (M.J.H.-F., J.D.) and for financial support. We also acknowledge the Patrimoine de l'Université de Liège and the Services de la Politique Scientifique. We are indebted to M. J. Heinesch for his highly valuable technical assistance.

Registry No. CH_3CN, 75-05-8; CH_3NC, 593-75-9.